Year: 2014

Soil formation rates on silicate parent material in alpine environments: Different approaches–different results?

Egli, Markus ; Dahms, Dennis ; Norton, Kevin

Abstract: High-mountain soils develop in particularly sensitive environments. Consequently, deciphering and predicting what drives the rates of soil formation in such environments are a major challenge. In terms of soil production or formation from chemical weathering, the predominating perception for high-mountain soils and cold environments is often that the chemical weathering 'portion' of soil development is temperature-inhibited, often to the point of non-occurrence. Several concepts exist to determine long-term rates of soil formation and development. We present three different approaches: (1) quantification of soil formation from minimally eroded soils of known age using chronosequences (known surface age and soil thickness — SAST), (2) determination of soil residence times (SRT) and production rates through chemical weathering using (un)stable isotopes (e.g. 230Th/234U activity ratios), and (3) a steady state approach using cosmogenic isotopes (e.g. 10Be). For each method, data from different climate zones, and particularly from high-mountains (alpine environment), are compared. The SAST and steady state approach give quite similar results for alpine environments (European Alps and the Wind River Range (Rocky Mountains, USA)). Using the SRT approach, soil formation rates in mountain areas (but having a temperate climate) do not differ greatly from the SAST and steady state approaches. Independent of the chosen approach, the results seem moderately comparable. Soil formation rates in high-mountain areas (alpine climate) range from very low to extremely high values and show a clear decreasing tendency with time. Very young soils have up to 3–4 orders of magnitude higher rates of development than old soils (105 to 106 yr). This apparently is a result of kinetic limits on weathering in regions having young surfaces and supply limits to weathering on old surfaces. Due to the requirement for chemical weathering to occur, soil production rates cannot be infinitely high. Consequently, a speed limit must exist. In the literature, this limit has been set at about 320 to 450 t/km2/a. Our results from the SAST approach show, however, that in alpine areas soil formation easily reaches rates of up to 800– 2000 t/km2/a. These data are consistent with previous studies in mountain regions demonstrating that particularly young soils intensively weather, even under continuous seasonal snowpack and, thus, that the concept of 'temperature-controlled' soil development (soil-forming intervals) in alpine regions must be reconsidered.

DOI: https://doi.org/10.1016/j.geoderma.2013.08.016

Originally published at:
Egli, Markus; Dahms, Dennis; Norton, Kevin (2014). Soil formation rates on silicate parent material in alpine environments: Different approaches–different results? Geoderma, 213:320-333.

DOI: https://doi.org/10.1016/j.geoderma.2013.08.016

Soil formation rates on silicate parent material in alpine environments: different approaches – different results?

Markus Egli[1]*, Dennis Dahms[2], Kevin Norton[3]

[1]Department of Geography, University of Zurich, CH-8057 Zurich, Switzerland

[2]Department of Geography, University of Northern Iowa, Cedar Falls, USA

[3]School of Geography, Environment and Earth Sciences (SGEES), Victoria University of Wellington, New Zealand

*Corresponding author. Tel.: +41 44 635 51 14; fax: +41 44 6356848.
E-mail address: markus.egli@geo.uzh.ch (M. Egli).

Abstract

High-mountain soils develop in particularly sensitive environments. Consequently, deciphering and predicting what drives the rates of soil formation in such environments is a major challenge. In terms of soil production or formation from chemical weathering, the predominating perception for high-mountain soils and cold environments is often that the chemical weathering 'portion' of soil development is temperature-inhibited, often to the point of non-occurrence. Several concepts exist to determine long-term rates of soil formation and development. We present three different approaches: (1) quantification of soil formation from minimally eroded soils of known age using chronosequences (known surface age and soil thickness - SAST), (2) determination of soil residence times (SRT) and production rates through chemical weathering using (un)stable isotopes (e.g. ^{230}Th / ^{234}U activity ratios), and (3) a steady state approach using cosmogenic isotopes (e.g. ^{10}Be). For each method, data from different climate zones, and particularly from high-mountains (alpine environment), are compared. The SAST and steady state approach give quite similar results for alpine environments (European Alps and the Wind River Range (Rocky Mountains USA)). Using the SRT approach, soil formation rates in mountain areas (but having a temperate climate) do not differ greatly from the SAST and steady state approaches. Independent of the chosen approach, the results seem moderately comparable. Soil formation rates in high-mountain areas (alpine climate) range from very low to extremely high values and show a clear decreasing tendency with time. Very young soils have up to 3 – 4 orders of magnitude higher rates of development than old soils (10^5 to 10^6 years). This apparently is a result of kinetic limits on weathering in regions having young surfaces and supply limits to weathering on old surfaces.

Due to the requirement for chemical weathering to occur, soil production rates cannot be infinitely high. Consequently, a speed limit must exist. In the literature, this limit has been set at about 320 to 450 t km^{-2} yr^{-1}. Our results from the SAST approach show, however, that in alpine areas soil formation easily reaches rates of up to 800 – 2000 t km^{-2} yr^{-1}. These data are consistent with previous studies in mountain regions demonstrating that particularly young soils intensively weather, even under continuous seasonal snowpack and, thus, that the concept of 'temperature-controlled' soil development (soil-forming intervals) in alpine regions must be reconsidered.

Kewords: soil formation, alpine regions, chronosequence, steady state, soil residence time

1. Introduction

As climate warming becomes a more obvious environmental factor, questions of how soils and landscapes have developed and what future scenarios may be possible are concerns of major scientific and socio-economic importance. This is especially important in high-mountain settings, where melting of permafrost and changing vegetation regimes lead to rapid and dramatic changes in soil formation and erosion (Haeberli, 2005; Haeberli et al., 2007). High mountain valleys experience active gravity-driven hillslope processes (Heimsath and McGlynn, 2008) - and this activity potentially increases when glaciers and permafrost retreat or frost periods decrease. Knowledge of the spatial and temporal dynamics of high mountain soil-development processes in a landscape context is therefore required; however, our current knowledge in this field is incomplete and fragmented. Predicting what drives the transition from 'non-soil' to a soil-mantled rocky landscape (or from bedrock or raw regolith to a 'developed' soil mantle) is, therefore, a significant challenge for models of landscape evolution and for 'critical zone' studies (Heimsath et al., 2012). The data needed to calculate weathering rates and the production of soil materials have recently become accessible through the use of cosmogenic or other nuclide techniques (e.g., Heimsath et al., 1997; Riebe et al., 2003, Dosseto et al., 2008; etc.). Likewise, evidence of material production or denudation is preserved in stream sediments or directly in soil profiles. Long-term total denudation rates can be measured at the catchment scale or single soil profile using (cosmogenic) nuclide measurements (e.g., Brown et al., 1995; Granger et al., 1996; von Blanckenburg, 2006). In combination with geochemical mass balance data from which dissolution losses are inferred from the rock-to-soil enrichment of insoluble elements, long-term chemical weathering rates can also be determined (Riebe et al., 2001, 2003, 2004a,b; Green et al., 2006; Norton and von Blanckenburg, 2010; see review by Granger and Riebe, 2012).

However, the determination of 'soil production' or 'soil formation' is difficult and several approaches and concepts exist that lead to potentially different or possibly even contradictory results. In this paper we compare three approaches for estimating soil production/formation rates, with particular focus on mountain and alpine areas where soils have developed in silicate materials of glacial moraines. These approaches include i) the chronosequence approach (stable sites, known surface age, profile thickness), ii) soil residence time, and iii) steady state approach (for details see section 3 below).

As the basic concepts behind of each these methods to determine rates of soil formation or production are distinctly different, it is useful to determine whether the results of these methods are also distinctly different - or not. In this paper we present and discuss these concepts by comparing published and new data from mountain sites having an alpine climate.

2. Soil formation and weathering

2.1. Principles

Landscapes are shaped by the uplift, deformation and breakdown of bedrock and the erosion, transport and deposition of sediment. According to Dietrich and Perron (2006), all landscapes must obey an equation for the conservation of mass:

$$\frac{\partial z}{\partial t} = U - I - \nabla q_s \qquad (1)$$

in which z is the elevation of the ground surface, t is time, U is the uplift rate, I is the lowering of the bedrock surface, and q_s is the volume flux of stored sediment (soil, colluvium, alluvium, and so on) per unit width. It is broadly understood that tectonic forcings influence the pace and pattern of landscape evolution by their control on landscape relief and the physical and chemical processes that move sediment and dissolve bedrock (West et al., 2005; Dixon et al., 2012). An understanding of the tectonic processes (U) operating on the landscape as well as 'geomorphic transport laws' (I and q_s) are required to describe the rates of different transport, bedrock-to-soil conversion and erosion processes in terms of material properties, climatic influences and attributes of the topography and subsurface.

Soil formation (or production) depends mainly on the lithology (e.g. highly reactive minerals such as carbonates and sulphates vs. crystalline rocks), the development of organic matter (Conen et al., 2007), the rate of supply of fresh regolith through physical weathering and erosion, the age of exposure, and the character of the hydrological system. This harkens back to the fundamental concept of Dokuchaev (1883) and, in an extended form, of Jenny (1941) according to which soil formation is a function of the five (more or less) independent factors 'time', 'climate', 'topography', 'organisms' and 'parent material'. All these factors act together to influence the rate(s) and direction(s) of soil formation. In this work, we focus on soils developed on silicate parent materials.

The terms 'soil production', 'soil formation' and 'soil development' have been used with differing meanings in different texts, and have to be defined in a first step. For the purposes of this paper, we consider the terms 'soil formation' and 'soil development' to be synonymous. The term 'soil production' designates the gross production while 'soil development (or soil formation)' describes the net effect.

- ***Soil formation*** (soil development; see Shaw (1930), Jenny (1941), Phillips (1993), Minasny et al. (2008), Sommer et al. (2008)): Soil is viewed as an open system with additions and removals of materials to and from the profile, and translocation, transformation within the profile. Pedogenesis can be progressive or regressive. Progressive pedogenesis includes processes that promote differentiated profiles leading to a horizonization, leaching, developmental upbuilding, and soil deepening. Regressive pedogenesis (Minasny et al., 2008, Sommer et al., 2008) includes processes that promote rejuvenation processes, retardant upbuilding (impedance produced by surface-accreted materials), and surface removals (erosion). In terms of soil thickness, soil formation (and as a synonym soil development) refers to a change (usually an increase) of h (Fig. 1). Soil formation is therefore considered as a net change in mass balance of the soil compartment.

- ***Soil production***: In general, soil production includes the transformation of the parent material into soil (due to chemical and physical weathering, mineral transformation) and the lowering of the bedrock (or parent material) – soil boundary (Heimsath et al., 1997). Ahnert (1967) and Heimsath et al. (1997) suggested that the rate of soil production ($\partial e / \partial t$) can be represented as an exponential decline with soil thickness, whereas other authors observed a humped function (e.g. Heimath et al., 2009).

2.2. Vegetation

Living organisms are important for many of soil and landscape related processes. Over short timescales, the impact of living organisms is quite apparent: rock weathering, soil formation and erosion, slope stability or instability and river dynamics are directly influenced by biotic processes that mediate chemical reactions, dilate soil, disrupt the ground surface, and add strength with a weave of roots (Dietrich and Perron, 2006). Tree root penetration plays an important role in rock wedging and fragmentation, as suggested by roots penetrating at depth within the cracked rock or saprolite and occasional wind throw (Scarciglia et al., 2007). Already at early stages, biologic activities such as lichen colonisation directly may affect rock weathering by physical (e.g. crack systems are intruded by lichens hyphae which cause rupture of primary minerals; Chen et al., 2000; Scarciglia et al., 2012) and additional chemical attack (e.g. excretion of organic acids that may promote dissolution and weathering; Adamo and Violante, 2000; Chen et al., 2000; Scarciglia et al., 2012). This finally leads to an enhanced mineral formation and transformation (Scarciglia et al., 2012).

Plant succession and the development of plant communities in high-mountain areas are tightly bound to the underlying substrate and other site factors (e.g. Burga et al., 2010; Frey et al., 2010). For example, retreating glaciers successively expose mineral substrates that are colonised within a few years by vascular plants, mosses, lichens and soil biota. At first sight, the small-scale vegetation pattern in proglacial areas with bare sediments or rocks (where vegetation is starting to grow) seems to be chaotic (Burga et al., 2010). Patterned structures may be associated with abrupt thresholds that either enhance or stop/hinder soil formation and vegetation development. This is due to microclimate, micro-relief, deposition of physically inhomogeneous parent material (sites with more fine-grained materials close to rock debris), disturbance and even to brief periglacial periods (cf. Haugland, 2004). At larger scales, patterns and processes are clearer and particular successions develop starting with one initial stage, followed by different development pathways and ending with coniferous forest as climax of the subalpine forest belt (Burga et al., 2010).

2.3. Chemical weathering, erosion, denudation

Chemical weathering includes the processes of mineral dissolution or alteration and transformation of initial mineral phases to those that are more stable at the earth's surface. Clay minerals are often a product of such near-surface weathering processes. The formation and stability of clay is dependent on both the precursor minerals and the ambient environmental conditions (Velde, 1995).

Limitations to silicate weathering generally include two different processes: *transport limitation* and *kinetic limitation*. The supply of water, acids and (organic) ligands relative to the supply of silicate minerals is large in *transport*-limited weathering regimes (West et al., 2005). Generally, old and flat topographies belong to this category. Where *kinetic* limitation is the main control on chemical weathering, silicate weathering ω depends on the kinetic rate of mineral dissolution W, the supply of material (e.g., by erosion) e, and the time t available for reaction (West et al., 2005)

$$\omega = W \cdot e \cdot t \qquad (2)$$

where the value W depends on environmental conditions such as temperature and runoff (or precipitation). Additionally, the weathering rate of a mineral or rock decreases with the time that the mineral spends in the weathering environment, as $\omega_V \propto t^{\lambda}$ with ω_V = instantaneous volumetric weathering rate, λ = (erosion) exponent (White and Brantley, 2003; West et al., 2005).

At both the catchment and profile scale, weathering rates can be determined through element depletion or accumulation obtained by mass balance studies (input-output budgets; e.g. April et al, 1986; Johnson and Lindberg, 1992; Wright et al., 1992; Bain et al., 1994; Drever, 1997; Olsson and Melkerud, 2000). The following mass balance techniques have commonly been applied to measure rates of chemical weathering (Porder et al., 2007):

(1) quantification of mass loss from minimally eroded soils of known age using chronosequences (Jenny, 1941; Taylor and Blum, 1995),

(2) catchment-scale river sampling (e.g. White and Blum, 1995; Riebe et al., 2004b),

(3) nuclide techniques (soil and catchment-wide; e.g. Heimsath et al., 1997) and

(4) laboratory experiments (e.g. White and Brantley, 2003).

While the latter method provides the opportunity to directly measure weathering rates of individual minerals, the time over which natural chemical weathering occurs (White and Hochella, 1992) can usually not be reproduced by experimental studies (see White and Brantley, 2003). Soil chronosequences and other approaches are therefore needed to estimate field weathering rates (element depletion rates, mineral transformation rates etc.; e.g. Föllmi et al., 2009a,b; Mavris et al., 2011 etc.) and also to permit the differentiation of surfaces of differing age (e.g. Fitze, 1982; Dahms, 2002, 2004). Weathering indices, chemical gradients, or clay mineral assemblages may differentiate soils even within a relatively narrow time range and provide information concerning processes at specific sites (Alexander and Burt, 1996; Birkeland, 1999; Evans, 1999; Righi et al., 1999; Egli et al., 2001, 2003). Additionally, cosmogenic and other nuclide techniques allow the determination of weathering, erosion, and denudation rates (see compilations in Anderson et al. (2007) and Dixon and von Blanckenburg (2012)).

In general, over centuries to millennia, the rates of primary mineral depletion and secondary clay and metal oxide formation progressively decrease with soil (surface) age (Taylor and Blum, 1995; Hodson et al., 1999; Stewart et al., 2001; White et al., 2009).

Rates of physical erosion and chemical weathering in many cases are positively correlated across diverse landscapes (Gaillardet et al., 1999; Dixon et al., 2009; etc.): up to a certain threshold value, increasing erosion causes increasing chemical weathering (Dixon et al., 2012). Areas of fast uplift have some of the highest global riverine solute fluxes (Gaillardet et al., 1999; Waldbauer and Chamberlain, 2005) and soil weathering rates (Riebe et al., 2001). These relationships suggest that tectonic uplift stimulates chemical weathering rates by increasing the supply of fresh minerals (Ferrier and Kirchner, 2009; Norton and von Blanckenburg, 2010; Dixon et al., 2012). Conversely, rapid uplift also may limit chemical weathering rates as erosion rates increase, soil residence times decrease, and weatherable minerals lack sufficient time to weather completely (Stallard and Edmond, 1983; Riebe et al., 2004a; West et al., 2005). In such cases, mineral weathering rates are limited by the kinetics of chemical reactions (Norton and von Blanckenburg, 2010; Dixon et al., 2012).

2.4. High-mountains and weathering

The general perception in terms of weathering in cold regions has been that mechanical processes predominate, with ‘freeze-thaw’ weathering as the prime agent. The assumption is that chemical processes are temperature-inhibited, even to the point of non-occurrence. However, many cold regions show similar or even more intense weathering assemblages than those in warmer regions (e.g. Hall et al., 2002; Föllmi et al., 2009a,b). Contrary to the temperature-inhibited assumption, several recent investigations document that weathering in cold Alpine regions, including chemical weathering, is most directly controlled by moisture availability (Egli et al., 2006). Furthermore, since weathering rates decrease with time of weathering (e.g. Egli et al., 2001; White and Brantley, 2003), the availability of fresh mineral surfaces that are provided by physical erosion influences/determines chemical weathering rates (White et al., 1999; Jacobson and Blum, 2003; Riebe et al., 2004b). Glaciers and glacial periods may have a significant impact on global weathering, changing the interplay between physical and chemical weathering processes by putting large volumes of dilute meltwaters and fine-grained sediments in contact with each other (Föllmi et al., 2009a,b; Arn et al., 2003). We see that the amount of mechanical denudation reported from glaciated valleys of Alaska, Norway and the Alps are an order of magnitude greater than those from equivalent non-glaciated basins (Hallet al., 1996; Föllmi et al., 2009b). Weathering is kinetically limited in regions having young surfaces (West et al., 2005). Proglacial areas and areas with young deposits in Alpine regions belong to this category.

Particularly in regions with solid bedrock as parent material, the available surface area of primary mineral grains increases until a certain maximum as far as weathering processes proceed. With time, weathering rates decrease again giving rise, under such conditions, to a ‘humped’ time-trend (see e.g. Humphreys and Wilkinson, 2007). The texture of the parent rock, and thus the available surface area, is an important factor in controlling the reaction rates (e.g., Taboada and García, 1999). Furthermore, microscale discontinuities such as twinning or breakage patterns along preferred lines that are structurally controlled by cleavage planes, joint fractures and any other crystallographic features may control silicate mineral weathering (Frazier and Graham, 2000; Scarciglia, et al., 2005). The increase in the pedogenic matrix may also promote a longer time of interaction of circulating soil water (in turn enhancing chemical reactions) with the soil system itself (e.g., Scarciglia et al., 2005, 2007). With increasing alteration, however, weathering intensity in soils is limited e.g. by dissolved Al-ions or precipitations of oxyhydroxides onto mineral surfaces that decrease the reaction rates (see e.g. Furrer et al., 1989; Sverdrup and Warfwinge, 1993, 1995), the availability of easily weatherable minerals, etc.

3. Techniques for the determination of soil formation rates

The diversity in soil landscapes at Earth's surface is the result, among other things, of the relationship between soil material production and erosion. Changes in soil material mass can be expressed by:

$$\frac{\partial(\rho_w h_w)}{\partial t} = \rho_r Q_{UA} - \nabla \cdot \left(\rho_w \vec{Q_D} \right) = \phi - \nabla q_e - \nabla q_w \qquad (3)$$

where ρ = bulk density (w: soil; r: parent material), h_w = soil material thickness, Q_{UA} = soil material mass production rate per unit area, Q_D = denudation mass flux rate per unit area, ϕ = soil production rate, q_e = soil erosion rate per unit area, q_w = chemical weathering rate per unit area (modified after Yoo et al., 2007; Yoo and Mudd, 2008).

In pedology we are frequently interested in how soil characteristics and processes change over time. Dynamic simulation models are based on the assumption that the state of each system at any moment can be quantified, and that changes in the state can be described by rate or differential equations (Hoosbeek et al., 2000). The new state, $state_{t+\Delta t}$, of the system is calculated according to

$$state_{t+\Delta t} = state_t + \Delta t(rate_t) \qquad (4)$$

From this new state ($state_{t+\Delta t}$) a new rate ($rate_{t+\Delta t}$) must be derived that can be used to calculate $state_{t+2t}$ and so on (= Euler's integration method). Numerical integration always yields some approximation of the true value. This concept seems simple: however, its accuracy depends on the calculation method and the length of Δt. Smaller time-steps give better solutions for non-linear soil evolution (see e.g. Sommer et al., 2008). Ideally, such models would be calibrated with empirically derived data.

The determination of the soil material production and formation rates in the field is associated with several difficulties and methodological limitations. The emergence of isotopic techniques over the last two decades (cosmogenic nuclides, U-series isotopes) now allows quantification of rates of geomorphic processes, which sheds new light on landscape and soil evolution.

Several general approaches exist for quantifying production/formation rates:

i) Known surface age and soil thickness (SAST) of undisturbed and stable sites (Table 1): This approach (using chronosequences) gives an 'integrated' soil formation rate as the soil is considered to be a 'black box'. Only the net effect that is due to an increase of soil thickness minus losses and/or plus gains can be calculated (Fig. 1). For this approach, erosion effects on stable landscape positions are considered as nearly negligible (see e.g. Egli et al., 2010a; Norton et al., 2010), so that soil and vegetation cover and/or a favourable topographic position drastically reduce erosion.

The soil thickness model was elaborated by Johnson et al. (2005), and adapted by Phillips et al. (2005). In principle, the following processes contribute to soil thickness (T):

$$T = (W + B) + (A + O + V) - (E + L + C_{surf} + C_{sub}) \qquad (5)$$

Upbuilding processes in the expanded soil thickness model include bedrock weathering (W), bioturbation (B), sediment accretion (A), organic matter accumulation (O), and volume expansion (V). Removal processes include surficial erosion and mass wasting (E), leaching (L), and surface consumption by fire, uptake, and harvesting (C_{surf}) and subsurface removals (C_{sub}) by the same processes. Soil development usually is regarded as nonlinear and is conceptualised by 'progressive' or 'regressive' process groups (Johnson and Watson-Steger, 1987; Sommer et al., 2008). By considering the soil as a black box only averaged and net values can be determined. Soil formation rates are calculated as soil thickness/soil age. Since this method integrates all soil development processes (progressive and regressive), it yields a minimum rate.

ii) Soil residence time (SRT) and production rates using (un)stable isotopes: e.g. ^{230}Th / ^{234}U activity ratios (Dosseto et al., 2008; 2011). Uranium disequilibrium analysis provides a new and independent tool by which to quantify the regolith production function in weathering profiles (Dosseto et al., 2008, 2011, 2012; Ma et al., 2010). The migration and change of the saprolite/soil boundary is independent from steady-state assumptions. This system takes advantage of disequilibrium between ^{230}Th and ^{234}U and ^{234}U and ^{238}U during weathering of primary minerals. Upon weathering, ^{234}U is lost from the soil to solution (U is much better soluble than Th), driving the system from secular equilibrium (leading to a relative enrichment of Th). The ^{238}U and ^{230}Th are then bound up in secondary clays or other weathering products, at which time ^{234}U begins to accumulate as ^{238}U weathers. The ratios of ^{230}Th/^{234}U and ^{234}U/^{238}U provide a measure of the time since secondary (clay)mineral development (i.e. soil formation). Soil production rates are derived from this method from the rate of downward migration of the soil/bedrock interface.

iii) Assuming steady state: Cosmogenic isotopes, such as beryllium-10, also are used to determine rates of soil production (e.g. Heimsath et al., 1997). However, this approach requires the assumption that soil erosion and production are balanced and that the soil thickness remains in steady-state. It has only been possible to test this hypothesis in a few instances (Heimsath et al., 2000). In steady-state conditions, the total denudation rate and the rate of soil formation (D_{soil}) are equal: $D = E + W = D_{soil}$. The concentration of cosmogenic nuclides in the topsoil or at the soil/bedrock interface is inversely related to the denudation rate of the surface such that rapid denudation (= soil formation at steady state) is associated with low nuclide concentrations and vice-versa. This approach enables the direct determination of overall soil production rates per unit time (e.g. Heimsath, 2006; Dixon et al., 2009, etc.), but the aggrading or degrading phases usually cannot be measured. Steady-state regolith or soil thickness, whereby surface removals approximately balance the production of new soil by bedrock weathering, is a common assumption of most models of hillslope and landscape evolution (Phillips, 2010). According to Phillips (2010), the assumption of steady-state conditions for soil, regolith, or weathering profile development may lead to unrealistic representations of the dynamics of pedogenesis and weathering profile evolution. However, Norton and von Blanckenburg (2010) showed that even in Alpine areas an approximate steady-state situation can be reached after 15 ky deglaciation.

4. Comparison of approaches and discussion

We compare published along with original data for soil production and formation rates obtained using the above three procedures. New soil formation data are from the European Alps and from the Wind River Range of Wyoming, USA (WRR) using soil chronosequences. We calculated soil formation rates from published soil data (e.g., Dahms et al., 2012; Egli et al., 2012) where information was available for soil thickness (by horizon), bulk density, and skeleton content, and where – for particularly young soils – a soil horizon could be identified with good conscience (the thickness of transition horizons such as BC, AC, etc. are counted half; Table 2; Sauer, 2010). Parent material is granitic glacial till at all the Wyoming sites, while soils of the Alps were mostly developed in granitoid till or relict rock glaciers (granitic material). Soil formation rates were estimated using the SAST approach. The corresponding data is given in Table 2. The main uncertainty with calculating soil production rates using this approach pertains to the soil skeleton material (> 2mm fraction). Is it part of the soil or not? Particles > 2 mm are usually considered 'chemically inert' for plant growth, although they can very well be the source of nutrients such as Ca, Mg and K (Ugolini et al., 2001).

In alpine areas, the soil skeleton mostly consists of primary silicates; consequently the production rates were calculated by subtracting the skeleton weight from the total soil mass. Using these datasets, we developed a weathering chronosequence of up to ~1 Ma (see also below). In general, the European sites have a moister climate (1100 – 2000 mm/yr precipitation) than the Wind River Range (from 1000 mm/yr in Stough Creek Basin to only 340 mm/yr in Sinks Canyon). Vegetation consists generally of pioneer plant communities, shrubs or grassland and montane forest, depending on the age and climatic zone of the deposits (Dahms et al., 2012). We show ranges of soil production rates based on the different approaches in Figure 2.

Using the *SAST approach*, the soil formation rates vary between 2 and 2600 t/km^2/a for the Alps and the Wyoming sites. We also used a similar dataset for Mediterranean soils compiled by Sauer (2010). Again, using the SAST approach, the range of soil formation rates varied through a similar range (1 – 4000 t/km^2/a).

Using the *soil residence time approach*, measured soil formation rates are between 9 and 832 t/km^2/a for all evaluated sites (data from Dosseto et al. (2008, 2011) and Ma et al. (2010)). Using the SRT approach, the alpine soils vary between 33 – 220 t/km^2/a, the temperate sites between 9 – 485 t/km^2/a, the subtropical (to temperate) between 14 – 832 t/km^2/a and the tropical between 65 – 622 t/km^2/a. Fewer observations were used for the SRT approach as not as many published data were available.

None of these approaches to measuring soil production/formation indicate that rates are lower in alpine areas (cold climates) than in other climates (e.g. temperate, Mediterranean or even tropical regions); rates of soil formation can reach extremely low but also extremely high values (Fig. 2, Table 2). Furthermore, the range of soil formation rates given by Small et al. (1999; derived from cosmogenic nuclides) for the Wind River Range, and by our calculations are similar, although the approaches are different (Fig. 2). In addition, the data presented by Norton et al. (2010) in the Alps appear to fit well with our SAST approach (Figs 2 and 3).

As one of few attempts to date, we are able to combine data from both alpine and temperate sites to relate rates of soil formation to soil age for up to ~1 Ma (Fig. 3). These data are shown in Table 3. Formation rates calculated using the SAST approach distinctly decrease with increasing age of the soil. In addition to our own alpine chronosequence data, we included alpine data from Peru (Goodman et al., 2001) and China (He and Tang, 2008) in our calculations (Figure 3). The data of Heimsath et al. (2001a) and Norton et al. (2010) represent the steady state approach and those of Ma et al. (2010) represent the SRT approach. While the negative trend within the steady state data (Figure 3) is due to a set relationship between cosmogenic nuclide-derived rates and apparent age, these data fit the independent data from the other methods. The dataset of Anderson et al. (2000) includes only data from solute chemistry. Erosion is assumed to have occurred also in the investigated catchments of the proglacial foreland of the Bench Glacier. We estimated soil production rates based on a steady state approach and assuming that *W* equals *E* (e.g. Dixon and von Blanckenburg, 2012; which probably underestimates soil formation in this case).

All data from the other two procedures – soil residence time (SRT) and apparent surface age (steady state approach) – fit nicely into this time trend. Consequently and independent of the chosen procedure, the results are comparable, lying in a similar range (order of magnitude) and show similar time trends.

In order to further investigate the role of climate in soil production, we compared the soil chronosequences from alpine regions to Mediterranean areas. We used an extensive data compilation of the temporal evolution of soils that have been developed on unconsolidated sediments on series of fluvial or marine sediments (Sauer, 2010), allowing us to calculate the corresponding soil formation rates (Table 4). Where soil density and soil skeleton (rock fragments) content were not available, they had to be estimated using the given soil descriptions. To complete the comparison, an example with volcanic terraces was included (Muhs, 1982). In Figure 4, we use the SAST approach to compare our soil formation rates as a function of time for alpine and Mediterranean sites. We show strongly decreasing soil formation rates with age for both of these regions (including the soils on volcanic material).

Trends in both are readily described by a power law. Apparently, in the early phases of pedogenesis, soil formation rates may be higher in Mediterranean than in alpine sites, with the highest rates in younger soils (< 10 ka). This, however, must not be true for all soil characteristics. According to Sauer (2010) and Sauer et al. (2010), most properties of Mediterranean soils exhibited the greatest changes during typical phases of soil development, *e.g.*, soil structure in soils < 10,000 y and rubification in soils > 100,000 y. The soils having an age of < 10ky have experienced only 1 warm phase (with some variations) whereas those having an age > 100 ky have experienced the Holocene warm phase and one or several other cold and warm phases during the Pleistocene. Apart from iron weathering and hematite formation processes, soil reddening also requires polygenesis with frequent secondary climatic oscillations under distinctly alternating moisture conditions. Consequently, the current Mediterranean climate alone is not sufficient for soil reddening (Wagner et al., 2013). Thus, separate rates of change in important soil properties need to be considered when looking for appropriate parameters to measure for the study of a particular chronosequence. The evidence that there are separate rates of change for different soil properties recalls Muhs' (1984) concept of the existence of 'intrinsic thresholds' that control many aspects of soil development.

Chemical weathering of primary minerals and the subsequent export of solutes is widely recognized to increase with increasing landscape erosion rates (Riebe et al., 2004b; West et al., 2005; Dixon et al., 2012; etc.). According to Dixon and von Blanckenburg (2012), this relationship can be explained by two processes: (1) erosion continually rejuvenates the landscape to supply fresh weatherable minerals from below to the surface; and (2) weathering reactions (e.g. freezing and thawing, chemical weathering that loosens rock particles etc.) alter rock to sustain physical processes of material production and erosion. However, very high production rates also are observed in areas with no or very low erosion (Fig. 3; Egli et al., 2010a). The compilation presented here shows that the highest production rates are on the youngest surfaces. Consequently, we must consider that weathering is kinetically limited (West et al., 2005) in regions with young 'fresh' moraine deposits, such as proglacial areas or areas with recent slope deposits in Alpine regions.

That the weathering-erosion relationship has certain 'speed limits' recently was demonstrated by Dixon and von Blanckenburg (2012). Ferrier and Kirchner (2008) also used a modelling approach to demonstrate that chemical denudation rates seem to reach a maximum at intermediate physical erosion rates. This implies that faster erosion rates may not lead necessarily to faster rates of chemical denudation; this also means that a certain maximum rate of material production cannot be exceeded. This is logical as the production rate cannot be infinitely high. Dixon and von Blanckenburg (2012) identified this 'speed limit' and estimated it to be between 320 to 450 t km^{-2} yr^{-1}. By using a different technique, the SAST approach, we demonstrate that soil production rate can even be higher; however, this is only possible when soil or surface age is < ~150 years, and soil production rates of up to 800 – 2000 t km^{-2} yr^{-1} might be possible in such cases. One possible reason for this discrepancy is that Dixon and von Blanckenburg (2012) most likely describe only the long-term (essentially only supply limited) rate limit, related to the long integration times of cosmogenic nuclide approaches. We must emphasise that the SAST method provides only minimum values. Erosion (that is assumed to be very low at stable sites) and particularly mass losses due to leaching (chemical weathering) are not included in the SAST analyses. The chemical weathering rate limit has been estimated to be 150 t km^{-2} yr^{-1} (Dixon and von Blanckenburg, 2012), so at least this value should be added to the obtained production rates when using the SAST approach.

A few caveats exist when deriving soil formation or production rates over time. It is typically assumed that soil forming parameters did not change through time such that the soils were generated under always the same conditions. In most of the world, soils are also influenced to some degree by dust influx. The higher the aridity is the more likely are aeolian inputs. To the extent that this influence leads to rejuvenation, it should be considered. The hillslopes of arid land hills and mountains are excellent dust traps, and in favourable conditions, accretionary and inflationary profile development promotes thick, vegetated and smooth soil-mantled hillsopes (McFadden, 2013). Where soils have developed for a known time-span, climatic conditions are often well defined. Over long time periods, however, climate conditions may have changed several times. Soils near a climatic boundary should experience a different climate more often than soils nearer the centre of a climatic region. Recent climate phase(s) also may have affected old and/or past soils and possibly have rejuvenated them by erosion processes (what finally gives rise to a polygenetic character of such soils). Likewise, microclimatic effects also influence weathering rates and pathways (Egli et al., 2010b). It is obvious that processes of soil formation proceed over time (Figs. 3 and 4); but the variability of soil formation/production over time must be explained by these above-mentioned factors and by the fact that some of the sites most likely experienced progressive and regressive evolutionary steps (cf. Johnson and Watson-Steger, 1987; Sommer et al., 2008).

5. Conclusions

Rates of soil material formation in alpine areas range from very low to extremely high values. These development rates strongly decrease with time: young soil materials weather up to 3 – 4 orders of magnitude faster than older soil materials (10^5 to 10^6 years). This relation corresponds with the concept of supply and kinetic limitation as controls on weathering. Weathering is kinetically controlled in regions with young geomorphic surfaces and supply limited on old geomorphic surfaces. The three approaches applied here to estimating the production of soil material by weathering (SAST, SRT and steady-state) have advantages and disadvantages. The SAST and SRT approaches more closely estimate net soil formation, whereas the steady-state approach estimates the gross formation rate (production rate) from regolith materials. Criticisms have accompanied the chronosequence approach from the beginning, including that, i.e., soils are of polygenetic, 'non-functional' nature, or many chronosequences are of less value for pedogenic interpretation due to their 'post-incisive' nature, which means different starting times of pedogenesis in the past, but continuous pedogenesis until recent times (Vreecken, 1975; Schaetzl and Anderson, 2005; Sommer et al., 2008; McFadden, 2013). However, this criticism would be also true for all other approaches, because for the SRT and steady-state approach, the overall rate (related to the whole residence time) or a rate in steady-state conditions (that must have been reached after a certain time of evolution) is calculated so that different rates are associated with different averaging times.

Although several soil chronosequences were used to calculate soil formation rates using the SAST approach, we were forced to estimate in some cases some of the parameters required for rate calculations (such as bulk density, proportion of rock fragments). Likewise, the assumption of a steady-state also may be problematic for many conditions (Phillips, 2010; McFadden, 2013).

However, independent of the approach used, the rate estimates are comparable and produce similar results (more or less). One important point to be considered is that soil formation can be progressive and also regressive (Sommer et al., 2008). The shown literature data and our own results however only give the overall value (without further specifying progressive or regressive trends). Since soil formation/production rates cannot be infinitely high, a speed limit of some kind must exist. The question is now - where this speed limit might be. According to Dixon and von Blanckenburg (2012), the limit seems to be between 320 to 450 t km^{-2} yr^{-1}. Our results show soil production rates in alpine areas are far higher, such that values of up to 800 – 2000 t km^{-2} yr^{-1} are possible.

6. Acknowledgements

We would like to thank Daniela Sauer and an unknown reviewer for their helpful comments on an earlier version of the manuscript.

References

Adamo, P., Violante, P., 2000. Weathering of rocks and neogenesis of minerals associated with lichen activity. Applied Clay Science 16, 229-256.

Ahnert, F., 1967. The role of the equilibrium concept in the interpretation of landforms of fluvial erosion and deposition. In: Macar, P. (ed.), L'évolution des versants, University of Liège, Liège, pp. 23-41.

Alexander, E.B., Burt, R., 1996. Soil development on moraines of Mendenhall Glacier, southeast Alaska. 1. The moraines and soil morphology. Geoderma 72, 1–17.

Alonso, P., Sierra, C., Ortega, E., Dorronsoro, C., 1994. Soil development indices of soils developed on fluvial terraces (Peñaranda de Bracamonte, Salamanca, Spain). Catena 23, 295–308.

Alonso, P., Dorronsoro, C., Egido, J. A., 2004. Carbonatation in palaeosols formed on terraces of the Tormes river basin (Salamanca, Spain). Geoderma 118, 261–276.

Anderson, S.P., Drever, J.I., Frost, C.D., Holden, P., 2000. Chemical weathering in the foreland of a retreating glacier. Geochim. Cosmochim. Acta 64, 1173–1189.

Anderson, S.P., von Blanckenburg, F., White, A.F., 2007. Physical and chemical controls on the critical zone. Elements, 3, 315-319.

Aniku, J. R. F., Singer, M. J., 1990. Pedogenic iron oxide trends in a marine terrace chronosequence. Soil Science Society of America Journal 54, 147–152.

April, R., Newton, R., Truettner Coles, L., 1986. Chemical weathering in two Adirondack watersheds: past and present-day rates. Geological Society of America Bulletin 97, 1232-1238.

Arn, K., Hosein, R., Föllmi, K.B., Steinmann, P., Aubert, D., Kramers, J., 2003. Strontium isotope systematics in two glaciated crystalline catchments: Rhone and Oberaar glaciers (Swiss Alps). Swiss Bulletin of Mineralogy and Petrology 83, 273–283.

Badía, D., Martí, C., Palacio, E., Sancho, C., Poch, R. M., 2009. Soil evolution over the Quaternary period in a semiarid climate (Segre river terraces, northeast Spain). Catena 77, 165–174.

Bain, D.C., Mellor, A., Wilson, M.J., Duthie, D.M.L., 1994. Chemical and mineralogical weathering rates and processes in an upland granitic till catchment in Scotland. Water, Air and Soil Pollution 73, 11 - 27.

Birkeland, P.W., 1999. Soils and geomorphology. 3rd edition, Oxford University Press, New York, 430 pp.

Bronk Ramsey, C., 2001. Development of the radiocarbon calibration program OxCal. Radiocarbon 43, 355-363.

Bronk Ramsey, C., 2009. Bayesian analysis of radiocarbon dates. Radiocarbon 51, 337-360.

Burga, C.A., Krüsi, B., Egli, M., Wernli, M., Elsener, S., Ziefle, M., Mavris, C., 2010. Plant succession and soil development on the foreland of the Morteratsch glacier (Pontresina, Switzerland): Straight forward or chaotic? Flora 205, 561-576.

Busacca, A. J., 1987. Pedogenesis of a chronosequence in the Sacramento Valley, California, U.S.A., I. Application of a soil development index. Geoderma 41, 123–148.

Calero, J., 2005. Génesis de la fracción mineral y de la ultramicrofábrica en una cronosecuencia de suelos sobre terrazas del río Guadalquivir. PhD Thesis. Universidad de Granada. Spain.

Calero, J., Delgado, R., Delgado, G., Martín-García, J. M., 2008. Transformation of categorical field soil morphological properties into numerical properties for the study of chronosequences. Geoderma 145, 278–287.

Chen, J., Blume, H.P., Beyer, L., 2000. Weathering of rocks induced by lichen colonization - a review. Catena 39, 121-146.

Conen, F., Yakutin, M.V., Zumbrunn, T., Leifeld, J., 2007. Organic carbon and microbial biomass in two soil development chronosequences following glacial retreat. European Journal of Soil Science 58, 758–762.

Dahms, D.E., 2002. Glacial Stratigraphy of Stough Creek Basin, Wind River Range, Wyoming. Geomorphology 42, 59-83.

Dahms, D.E., 2004. Relative and numeric age data for Pleistocene glacial deposits and diamictons in and near Sinks Canyon, Wind River Range, Wyoming, U.S.A. Arctic, Antarctic, and Alpine Research 36, 59-77.

Dahms, D. Favilli, F., Krebs, R., Egli, M., 2012. Soil weathering and accumulation rates of oxalate-extractable phases from alpine chronosequences of up to 1 Ma in age. Geomorphology, 151-152, 99-113.

Dequincey, O., Chabaux, F., Clauer, N., Sigmarsson, O., Liewig, N., Leprun, J.-C., 2002. Chemical mobilizations in laterites: Evidence from trace elements and ^{238}U–^{234}U–^{230}Th disequilibria. Geochim. Cosmochim. Acta 66, 1197–1210.

Dietrich, W.E., Perron, J.T., 2006. The search for a topographic signature of life. Nature 439, 411–418.

Dixon, J.L., Heimsath, A.M., Amundson, R., 2009. The critical role of climate and saprolite watheirng in landscape evolution. Earth Surface Processes and Landforms 34, 1507-1521.

Dixon, J.L., von Blanckenburg, F., 2012. Soils as pacemakers and limiters of global silicate weathering. Comptes Rendus Geoscience 344, 596-609.

Dixon, J.L.,Hartshorn, A.S., Heimsath, A.M., DiBiase, R.A., Whipple, K.X., 2012. Chemical weathering response to tectonic forcing: A soils perspective from the San Gabriel Mountains, California. Earth and Planetary Science Letters 323-324, 40-49.

Dokuchaev, V. V. 1883. Russian Chernozem. In: Kaner, N. (ed.), Selected works of V. V. Dokuchaev (1967). Jerusalem, Int. Program Sci. Transl., p. 1–419.

Dorronsoro, C., Alonso, P., 1994. Chronosequence in Almar River, fluvial terrace soil. Soil Science Society of America Jourbak 58, 3, 910–925.

Dosseto, A., Turner, S., Buss, H.L., Chabaux, F., 2007. The timescale of sediment transport in a small tropical watershed. Geochim. Cosmochim. Acta 71 (Suppl. 15), A972.

Dosseto, A., Turner, S.P., Chappell, J., 2008. The evolution of weathering profiles through time: new insights from uranium-series isotopes. Earth Planetary Science Letters 274, 359–371.

Dosseto, A., Buss,H., Suresh, P.O., 2011. The delicate balance between soil production and erosion, and its role on landscape evolution. Applied Geochemistry 26, S24-S27.

Dosseto, A., Buss,H., Suresh, P.O., 2012. Rapid regolith formation over volcanic bedrock and implications for landscape evolution. Earth and Planetary Science Letters 37-338, 47-55.

Drever, J.I., 1997. Catchment mass balance. In: Saether O.M., de Caritat, P. (eds), Geochemical Processes, Weathering and Groundwater Recharge in Catchments, Balkema, Rotterdam, pp. 241 - 261.

Egli, M., Fitze, P., Mirabella, A,. 2001. Weathering and evolution of soils formed on granitic, glacial deposits: results from chronosequences of Swiss alpine environments. Catena 45, 19-47.

Egli, M., Mirabella, A., Fitze, P., 2003. Formation rates of smectites derived from two Holocene chronosequences in the Swiss Alps. Geoderma 117, 81-98.

Egli, M., Wernli, M., Kneisel, C., Haeberli, W., 2006. Melting glaciers and soil development in the proglacial area Morteratsch (Swiss Alps): I Soil type chronosequence. Arctic, Antarctic, and Alpine Research 38, 499-509.

Egli, M., Brandová, D., Böhlert, R. Favilli, F., Kubik, P., 2010a. ^{10}Be inventories in Alpine soils and their potential for dating land surfaces. Geomorphology 119, 62-73.

Egli, M., Sartori, G., Mirabella, A., 2010b. The effects of exposure and climate on the weathering of late Pleistocene and Holocene Alpine soils. Geomorphology 114, 466-482.

Egli, M., Favilli, F., Krebs, R., Pichler, B., Dahms, D., 2012. Soil organic carbon and nitrogen accumulation rates in cold and alpine environments over 1 Ma. Geoderma, 183-184, 109-123.

Eppes, M. C., Bierma, R., Vinson, D., Pazzaglia, F., 2008. A soil chronosequence study of the Reno valley, Italy: Insights into the relative role of climate versus anthropogenic forcing on hillslope processes during the mid-Holocene. Geoderma 147, 97–107.

Evans, D.J.A., 1999. A soil chronosequence from neoglacial moraines in western Norway. Geografiska Annaler 81A, 47–62.

Ferrier, K.L., Kirchner, J.W., 2008. Effects of physical erosion on chemical denudation rates: A numerical modeling study on soil-matled hillslopes. Earth and Planetary Science Letters 272, 591-599.

Fitze, P., 1982. Zur Relativdatierung von Moränen aus Sicht der Bodenentwicklung in den kristallinen Zentralalpen. Catena 9, 265-306.

Föllmi, K.B., Arn, K., Hosein, R., Adatte, T., Steinmann, P., 2009a. Biogeochemical weathering in sedimentary chronosequences of the Rhône and Oberaar Glaciers (Swiss Alps): rates and mechanisms of biotite weathering. Geoderma 151, 270-281.

Föllmi, K.B., Hosein, R., Arn, K., Steinmann, P., 2009b. Weathering and the mobility of phosphorus in the catchments and forefields of the Rhône and Oberaar glaciers, central Switzerland: Implications for the global phosphorus cycle on glacial-interglacial timescales. Geochimica et Cosmochimica Acta 73, 2252-2282.

Frazier, C.S., Graham, R.C., 2000. Pedogenic transformation of fractured granitic bedrock, southern California: Soil Science Society of America Journal 64, 2057-2069.

Frey, B., S.R. Rieder, I. Brunner, M. Plotze, S. Koetzsch, A. Lapanje, H. Brandl, G. Furrer. 2010. Weathering-associated bacteria from the Damma Glacier forefield: Physiological capabilities and impact on granite dissolution. Applied and Environmental Microbiology 76, 4788–4796.

Furrer, G., Westall, J., Sollins, P., 1989. The study of soil chemistry through quasi-steady-state models: I. Mathematical definition of the model. Geochimica et Cosmochimica Acta 53, 595–601.

Gaillardet, J., Dupré, B., Louvat, P., Allègre, C.J., 1999. Global silicate weathering and CO_2 consumption rates deduced from the chemistry of large rivers. Chemical Geology 159, 11018.

Goodman, A.Y., Rodbell, D.T., Seltzer, G.O., Mark, B.G., 2001. Subdivision of glacial deposits in southeastern Peru based on pedogenetic development and radiometric ages. Quaternary Research, 56, 31-50.

Granger, D.E., Riebe, C.S., 2012. Cosmogenic Nuclides in Weathering and Erosion. In: Treatise on Geochemistry, Volume 5: Surface and Ground Water, Weathering, and Soils. (2nd edition). In press.

Green, E.G., Dietrich, W.E., Banfield, J.F., 2006. Quantification of chemical weathering rates across an actively eroding hillslope. Earth and Planetary Science Letters, 242, 155-169.

Haeberli, W., 2005. Climate change and glacial/periglacial geomorphodynamics in the Alps: A challenge of historical dimensions. Geografia Fisica e Dinamica Quaternaria SUPPL. 7, 9-14.

Haeberli, W., Egli, M., Keller, F., Krüsi, B., Rothenbuehler, C., Meilwes, J., Gruber, S., 2007. Raum-zeitliche Informationen über schnelle Klimaänderungen in hochalpinen Umweltsystemen als strategisches Werkzeug für Analyse, Kommunikation, partizipative Planung und Managment im Tourismusgebiet Oberengadin. Schlussbericht GISALP, NFP48 (Nationales Forschungsprogramm „Alpen“). vdf-Verlag, Zürich.

Hall, K., Thorn, C.E., Matsuoka, N., Prick, A., 2002. Weathering in cold regions: some thoughts and perspectives. Progress in Physical Geography 26, 577-603.

Hallet, B., Hunter, L., Bogen, J., 1996. Rates of erosion and sediment evacuation by glaciers: a review of field data and their implications. Global and Planetary Change 12, 213–235.

Harden, J. W., 1982. A quantitative index of soil development from field descriptions: examples from a chronosequence in central California. Geoderma, 28, 1-28.

Harden, J. W., Sarna-Wojcicki, A. M., Dembroff, G. R., 1986. Soils developed on coastal and fluvial terraces near Ventura, California. U.S. Geological Bulletin, 1590-B, series: Soil chronosequences in the Western United States, United States Government Printing Office, Washington.

Harrison, J. B. J., McFadden, L. D., Weldon III, R. J., 1990. Spatial soil variability in the Cajon Pass chronosequence: implications for the use of soils as a geochronological tool. Geomorphology 3, 399–416.

Haugland, J.E., 2004. Formation of patterned ground and fine-scale soil development within two late Holocene glacial chronosequences: Jotunheimen, Norway. Geomorphology 61, 287–301.

He, L., Tang, Y., 2008. Soil development along primary succession sequences on moraines of Hailuogou Glacier, Gongga Mountain, Sichuan, China. Catena 72, 259-269.

Heimsath AM. 2006. Eroding the land: steady-state and stochastic rates and processes through a cosmogenic lens. GSA Special Paper 415: 111–129. DOI: 10.1130/2006.2415(07).

Heimsath, A.M., McGlynn, R., 2008. Quantifying periglacial erosion in the Nepal high Himalaya. Geomorphology 97, 5-23.

Heimsath, A. M., Dietrich, W. E., Nishiizumi, K., Finkel, R. C., 1997. The soil production rate function and landscape equilibrium. Nature 388, 358-361.

Heimsath, A.M., Chappell, J., Dietrich,W.E., Nishizumi, K., Finkel, R.C., 2000. Soil production on a retreating escarpment in southeastern Australia. Geology 28, 787–790.

Heimsath, A.M., Chapell, J., Dietrich, W.E., Nishiizumi, K, Finkel, R.C., 2001a. Late Quaternary erosion in southeastern Australia: a field example using cosmogenic nuclides. Quaternary International 83–85, 169–185.

Heimsath, A.M., Dietrich, W.E., Nishiizumi, K, Finkel, R.C., 2001b. Stochastic processes of soil production and transport: erosion rates, topographic variation and cosmogenic nuclides in the Oregon coast range. Earth Surface Processes and Landforms 26, 531-552.

Heimsath, A.M., Jon, D., Dietrich, W.E., 2005. The illusion of diffusion: Field evidence for depth-dependent sediment transport. Geology 33, 949-952.

Heimsath, A.M., Fink, D., Hancock, G.R., 2009. The 'humped' soil production function: eroding Arnhem Land, Australia. Earth Surface Processes and Landforms 34, 1674-1684.

Heimsath, A.M., DiBiase, R.A., Whipple, K.X., 2012. Soil production limits and the transition to bedrock-dominated landscapes. Nature Geoscience 5, 210–214.

Hodson, M.E., Langan, S.J., Simon, J., 1999. The influence of soil age on calculated mineral weathering rates. Applied Geochemistry 14, 387– 394.

Hoosbeek, M. R., Amundson, R. G., Bryant, R. B., 2000. Pedological Modeling. In: Sumner, M.E. (ed.), Handbook of Soil Science. CRC Press, Boca Ratons, pp. E77-120.

Humphreys, G.S., Wilkinson, M.T., 2007. The soil production function: A brief history and its re-discovery. Geoderma 139, 73–78

Jacobson, A.D., Blum, J.D., 2003. Relationship between mechanical erosion and CO_2 consumption in the New Zealand Southern Alps. Geology 31, 865–868.

Jenny, H., 1941. Factors of soil formation. Mc Graw-Hill Book Company, New York.

Johnson, D.L., Watson-Stegner, D., 1987. Evolution model of pedogenesis. Soil Sci. 143, 349–366.

Johnson, W., Lindberg, E., 1992. Atmospheric deposition and forest nutrient cycling: a synthesis of the Integrated Forest Study. Springer Verlag, New York.

Johnson, D.L., Domier, J.E.J., Johnson, D.N., 2005. Animating the biodynamics of soil thickness using process vector analysis: a dynamic denudation approach to soil formation. Geomorphology 67, 23–46.

Ma, L., Chabaux, F., Pelt, E., Blaes, E., Jin, L., Brantley, S., 2010. Regolith production rates calculated with uranium-series isotopes at Susquehanna/Shale Hills Critical Zone Observatory. Earth and Planetary Science Letters 297, 211-225.

Mathieu, D., et al., 1995. Short-lived U and Th isotope distribution in a tropical laterite derived from granite (Pitinga river basin, Amazonia, Brazil): application to assessment of weathering rate. Earth and Planetary Science Letters 136, 703–714.

Mavris, C. Plötze, M., Mirabella, A., Giaccai, D., Valboa, G., Egli, M., 2011. Clay mineral evolution along a soil chronosequence in an Alpine proglacial area. Geoderma, 165, 106-117.

McFadden, L.D., 2013, Strongly dust-influenced soils and what they tell us about landscape dynamics in vegetated aridlands of the southwestern United States. In: Bickford, M.E. (ed.), The Web of Geological Sciences: Advances, Impacts, and Interactions: Geological Society of America Special Paper 500, chapter 15, doi:10.1130/2013.2500(15).

McFadden, L. D., Weldon, R. J., 1987. Rates and processes of soil development on Quaternary terraces in Cajon Pass, southern California. Geological Society of America Bulletin 98, 280–293.

Meixner, R. E., Singer, M. J., 1981. Use of a field morphology rating system to evaluate soil formation and discontinuities. Soil Science 131, 2, 114–123.

Merritts, D. J., Chadwick, O. A., Hendricks, D. M. (1991). Rates and processes of soil evolution on uplifted narine terraces, Northern California. Geoderma 51, 241–275.

Minasny, B., MCBratney, A.B., Salvador-Blanes, S., 2008. Quantitative models for pedogenesis – A review. Geoderma 144, 140-157.

Muhs, D., 1982. A soil chronosequence on Quaternary marine terraces, San Clemente Island, California. Geoderma 28, 257-283.

Muhs, D., 1984. Intrinsic Thresholds in Soil Systems. Physical Geography 5, 99-110.

Norton, K.P., von Blanckenburg, F., 2010. Silicate weathering of soil mantled slopes in an active Alpine landscape. Geochim. Cosmochim. Acta. 74, 5243–5258.

Norton, K.P., von Blanckenburg, F., Kubik, P.W., 2010. Cosmogenic nuclide-derived rates of diffusive and episodic erosion in the glacially sculpted upper Rhone Valley, Swiss Alps. Earth Surface Processes and Landforms 35, 651–662.

Olsson, M.T., Melkerud P.-A., 2000. Weathering in three podzolized pedons on glacial deposits in northern Sweden and central Finland. Geoderma 94, 149-161.

Phillips, J.D., 2010. The convenient fiction of steady-state soil thickness. Geoderma 156, 389-398.

Phillips, J.D., Marion, D.A., Luckow, K., Adams, K.R., 2005. Nonequilibrium regolith thickness in the Ouachita Mountains. Journal of Geology 113, 325–340.

Porder, S., Hilley, G.E., Chadwick, O.A., 2007. Chemical weathering, mass loss, and dust inputs across a climate by time matrix in the Hawaiian Islands. Earth and Planetary Science Letters 258, 414-427.

Reimer, P.J., Baillie, M.G.L., Bard, E., Bayliss, A., Beck, J.W., Blackwell, P.G., Bronk Ramsey, C., Buck, C.E., Burr, G.S., Edwards, R.L., Friedrich, M., Grootes, P.M., Guilderson, T.P., Hajdas, I., Heaton, T.J., Hogg, A.G., Hughen, K.A., Kaiser, K.F., Kromer, B., McCormac, F.G., Manning, S.W., Reimer, R.W., Richards, D.A., Southon, J.R., Talamo, S., Turney, C.S.M., van der Plicht, J., Weyhenmeyer, C.E., 2009. INTCAL09 and MARINE09 radiocarbon age calibration curves, 0-50,000 years cal BP. Radiocarbon 51, 1111-1150.

Riebe, C.S., Kirchner, J.W., Granger, D.E., Finkel, R.C., 2001. Strong tectonic and weak climatic control of long-term chemical weathering rates. Geology 29, 511–514.

Riebe, C. S., Kirchner, G., Finkel, R. C., 2003. Long-term rates of chemical weathering and physical erosion from cosmogenic nuclides and geochemical mass balance. Geochimica et Cosmochimica Acta 67, 4411-4427.

Riebe, C.S., Kirchner, J.W., Finkel, R.C., 2004a. Sharp decrease in long-term chemical weathering rates along an altitudinal transect. Earth and Planetary Science Letters 218, 421-434.

Riebe, C.S., Kirchner, J.W., Finkel, R.C., 2004b. Erosional and climatic effects on long-term chemical weathering rates in granitic landscapes spanning diverse climate regimes. Earth and Planetary Science Letters 224, 547-562.

Righi, D., Huber, K., Keller, C., 1999. Clay formation and podzol development from postglacial moraines in Switzerland. Clay minerals 34, 319-332.

Sauer, D., 2010. Approaches to quantify progressive soil development with time in Mediterranean climate—I, Use of field criteria. Journal of Plant Nutrition and Soil Science 173, 822–842.

Sauer, D., Wagner, S., Brückner, H., Scarciglia, F., Mastronuzzi, G., Stahr, K., 2010. Soil development on marine terraces near Metaponto (Gulf of Taranto, southern Italy). Quaternary International 222, 48-63.

Scarciglia, F., Le Pera, E., Critelli, S., 2005. Weathering and pedogenesis in the Sila Grande Massif (Calabria, South Italy): from field scale to micromorphology. Catena 61, 1-29.

Scarciglia, F., Le Pera, E., Critelli, S., 2007. The onset of the sedimentary cycle in a midlatitude upland environment: weathering, pedogenesis and geomorphic processes on plutonic rocks (Sila Massif, Calabria). In: Arribas, J., Critelli, S., Johnsson, M.J. (eds.), Sedimentary provenance and petrogenesis: perspectives from petrography and geochemistry: Geological Society of America, Special Paper 420, pp. 149-166.

Scarciglia, F., Saporito, N., La Russa, M.F., Le Pera, E., Macchione, M., Puntillo, D., Crisci, G.M., Pezzino, A., 2012. Role of lichens in weathering of granodiorite in the Sila uplands (Calabria, southern Italy). Sedimentary Geology 280, 119-134.

Schaetzl, R.J., Anderson, S., 2005. Soils: Genesis and Geomorphology. Cambridge University Press, Cambridge.

Small, E.E., Anderson, R.S., Hancock, G.S., 1999. Estimates of the rate of regolith production using 10Be and 26Al from an alpine hillslope. Geomorphology 27, 131-150.

Sommer, M., Gerke, H.H., Deumlich, D., 2008. Modelling soil landscape genesis – A "time split" approach for hummocky agricultural landscapes. Geoderma 145, 480-493.

Stallard, R.F., Edmond, J.M., 1983. Geochemistry of the Amazon: II. The influence of the geology and weathering environment in the dissolved load. J. Geophys. Res. 88, 9671–9688.

Stewart, B.W., Capo, R.C., Chadwick, O.A., 2001. Effects of rainfall on weathering rate, base cation provenance, and Sr isotope composition of Hawaiian soils. Geochimica et Cosmochimica Acta 65, 1087– 1099.

Sverdrup, H., Warfvinge, P., 1993. Calculating field weathering rates using a mechanistic geochemical model PROFILE. Journal of Applied Geochemistry 8, 273 - 283.

Sverdrup, K., Warfvinge, P., 1995. Estimating field weathering rates using laboratory kinetics. In: White, A.F., Brantley, S.L. (eds.), Chemical Weatheing Rates of Silicate Minerals. Reviews in Mineralogy, vol. 31. Mineral. Soc. Amer., Washington, D.C., pp. 485– 541.

Taylor, A., Blum, J.D., 1995. Relation between soil age and silicate weathering rates determined from the chemical evolution of a glacial chronosequence. Geology 23, 979– 982.

Ugolini, F.C., Corti, G., Dufey, J.E., Agnelli, A., Certini, G., 2001. Exchangeable Ca, Mg, and K of rock fragments and fine earth from sandstone and siltstone derived soils and their availability to grass. Journal of Plant Nutrition and Soil Science 164, 309-315.

Velde, B., 1995. Origin and mineralogy of clays. Clays and the Environment. Springer- Verlag, Berlin Heidelberg, Germany.

von Blanckenburg, F., 2006. The control mechanisms of erosion and weathering at basin scale from cosmogenic nuclides in river sediment. Earth and Planetary Science Letters 242, 224-239.

Vreecken, W.J., 1975. Principal kinds of chronosequences and their significance in soil history. Journal of Soil Science 26, 378–394.

Waldbauer, J.R., Chamberlain, C.P., 2005. Influence of uplift, weathering and base cation supply on past and future CO_2 levels. In: Ehleringer, J.R., Cerling, T.E., Dearing, M.D. (Eds.), History of Atmospheric CO_2 and Its Effects on Plants, Animals and Ecosystems. Springer Verlag, Berlin, pp. 166–184.

Wagner, S., Eckmeier, E., Skowronek, A., Günster, N., 2013. Quaternary paleosols and sediments on the Balearic Island as indicators of climate change. Catena, http://dx.doi.org/10.1016/j.catena.2013.06.022

West, A.J., Galy, A., Bickle, M., 2005. Tectonic and climatic controls on silicate weathering. Earth and Planetary Science Letters 235, 211–228.

White, A.F., Hochella Jr., M.F., 1992. Surface chemistry associated with the cooling and subaerial weathering of resent basalt flows. Geochimica et Cosmochimica Acta 56, 3711 –3721.

White, A.F., Blum, A.E., 1995. Effects of climate on chemical weathering in watersheds. Geochimica et Cosmochimica Acta 59, 1729–1747.

White, A.F., Brantley, S.L., 2003. The effect of time on the weathering of silicate minerals: why do weathering rates differ in the laboratory and field? Chemical Geology 202, 479-506.

White, A.F., Blum, A.E., Bullen, T.D., Vivit, D.V., Schulz, M., Fitzpatrick, J., 1999. The effect of temperature on experimental and natural chemical weathering rates of granitoid rocks. Geochimica et Cosmochimica Acta 63, 3277–3291.

White, A.F., Schulz, M.S., Stonestrome, D.A., Vivit, D.V., Fitzpatrick, J., Bullen, T.D., Maher, K., Blum, A.E., 2009. Chemical weathering of a marine terrace chronosequence, Santa Cruz, California. Part II: Solute profiles, gradients and the comparisons of contemporary and long-term weathering rates. Geochimica et Cosmochimica Acta 73, 2769–2803.

Wright, R.F., Lotse, E., Semb, A., 1994. Experimental acidification of alpine catchments at Sogndal, Norway: results after 8 years. Water, Air and Soil Pollution 72, 297 - 315.

Yoo, K., R. Amundson, A.M. Heimsath, W.E. Dietrich, G.H. Brimhall, 2007. Integration of geochemical mass balance with sediment transport to calculate rates of soil chemical weathering and transport on hillslopes. J. Geophys. Res. 112:F02013. doi:10.1029/2005JF000402

Yoo, K., Mudd, S.M., 2008. Toward process-based modelling of geochemical soil formation across diverse landforms: A new mathematical framework. Geoderma 146, 248-260.

Table 1. Short description of methods for soil production rate determination. With D_{soil} = Soil conversion rate; E = physical erosion, W = chemical weathering, h = soil thickness, t = time

Method	Notations	References
Surface age – profile thickness (SAST)	Age constraints due to dated surfaces (e.g. moraines). Calculation of soil formation rates (stable sites) by relating soil profile thickness to surface age: $D_{soil} = \frac{h}{t}$	Given in its principles e.g. in Jenny, 1941; Harden, 1982, Taylor and Blum, 1995; Johnson et al., 2005; etc.
Soil residence time (SRT)	Calculation of the time elapsed since conversion from bedrock to soil in each horizon of a weathering profile. U-series isotopes in weathering profiles: their abundance varies with time as a function of radioactive decay, loss through mineral dissolution and gain through either illuviation, dust deposition or both	Mathieu et al., 1995; Dosseto et al., 2008, 2011, 2012; Ma et al., 2010, etc.
Steady state approach	$D = E+W = D_{soil}$. Determination of total denudation (D) using cosmogenic nuclides.	Heimsath et al., 1997, 2000; Riebe et al., 2003, 2004, Dixon and von Blanckenburg, 2012, etc.

Table 2
Click here to download Table: Table2.doc

Table 2. Basic data and calculation of soil formation rates of sites in the European Alps and the Rocky Mountains (Wind River Range).

Site/Profile	Soil age	Soil thickness whole soil	Soil thickness[1)] A/B/E/O+1/2(AC/CA/BC/CB/OC)	Formation rates[2)]	Average bulk density[2)]	Skeleton proportion[2)]	Soil formation rates[2),3)] skeleton not considered	Soil formation rates[2),4)] skeleton considered
	a	cm	cm	mm/a	g/cm3	%	$t/km^2/a$	$t/km^2/a$
A) European Alps								
Morteratsch	138	14	12	0.83	0.87	46	725	361
	128	40	25	1.95	1.46	66	2852	956
	108	15	9	0.83	1.50	65	1250	424
	98	5	3	0.31	1.40	52	429	207
	68	4	4	0.59	1.33	3	1691	765
	48	2.5	3	0.63	1.60	64	1000	360
	48	4	4	0.83	1.40	26	1167	863
	58	12	12	2.07	1.00	63	2069	766
	73	10	7	0.89	1.04	55	925	367
	78	10	18	2.24	1.57	73	3532	898
	35	4	2	0.57	1.40	53	800	376
	35	4	2	0.57	1.40	66	800	272
	35	4	2	0.57	1.40	77	800	184
	30	4	2	0.67	1.40	53	933	439
	30	4	2	0.67	1.40	66	933	317
	20	4	2	1.00	1.40	77	1400	322
	3	4	2	6.67	1.40	75	9333	2333
	3	4	2	6.67	1.40	72	9333	2613
	140	25	25	1.79	1.76	61	3143	1247
	140	8	4	0.29	1.00	11	286	254
	120	3	3	0.25	1.50	40	375	225
	100	2	2	0.20	1.50	40	300	180
	80	6	5	0.63	1.34	49	838	393
	70	3	3	0.43	1.30	40	557	334
	60	12	6	1.00	1.50	55	1500	675
	30	6	3	1.00	1.40	70	1500	705
	30	15	8	2.50	1.60	66	4000	1360
	20	18	9	4.50	1.80	77	8100	1863
	12460	105	88	0.07	1.55	50	109	53
	1300	45	38	0.29	1.20	40	346	200

Gletsch, Schmadri	150	15	10	0.67	1.16	37	773	481
	260	25	20	0.77	1.19	45	912	497
	300	25	20	0.67	1.30	55	863	339
	450	35	30	0.67	1.02	59	681	273
	700	45	40	0.57	0.98	40	559	338
	3000	45	45	0.15	1.03	49	155	65
	10500	105	100	0.10	1.34	50	128	61
	3300	70	70	0.21	1.47	53	311	123
	11500	95	88	0.08	1.30	21	107	76
Val Mulix	14900	70	60	0.04	1.30	41	52	25
	10000	60	60	0.06	1.56	67	94	30
	10700	60	43	0.04	0.94	48	38	17
	9600	50	31	0.03	1.14	46	35	16
	8600	35	40	0.05	0.87	48	40	17
Val di Rabbi	17311	60	53	0.03	1.06	34	32	20
	11106	40	40	0.04	1.18	35	43	26
	10754	30	20	0.02	1.06	28	20	14
	8860	40	40	0.05	0.93	16	42	35
	10837	50	50	0.05	1.20	29	55	37
	4729	60	53	0.11	1.12	61	125	47
	5452	60	55	0.10	1.28	50	129	64
	9203	48	37	0.04	1.08	45	43	23
	11197	40	32	0.03	1.15	28	32	23
Meggerwald	19200	130	100	0.05	1.21	12	63	54
	19200	130	105	0.05	1.30	18	71	58
B) Wind River Range								
	150	25	10	0.65	1.35	42	225	131
	1500	30	16	0.11	1.72	48	183	95
	9930	45	33	0.03	1.32	24	43	32
	12930	75	49	0.04	1.43	33	54	35
	14500	90	55	0.04	1.44	36	54	34
	16000	85	57	0.04	1.30	26	46	33
	16000	75	63	0.04	1.32	27	51	37
	22000	50	40	0.02	1.46	31	27	18
	65000	85	68	0.01	1.59	27	17	12

130000	100	93	0.01	1.56	15	11	9
630000	210	170	0.00	1.59	16	4	4
850000	150	150	0.00	1.51	33	3	2
1200000	500	385	0.00	1.56	12	5	5

[1] According to Dorronsoro and Alonso (1994) and Sauer (2010) including combinations (considered as whole horizon) of BE, AE etc.; O: the Oa horizon is considered

[2] Related to a soil thickness of the horizons A/B/E+1/2(AC/CA/BC/CB)

[3] Formation rates calculated based on the whole soil mass

[4] Fomration rates calculated based on the soil mass minus skeleton content

Table 3
Click here to download Table: Table3.doc

Table 3. Compiled datasets of soil formation rates in alpine and temperate climate zones as a function of time.

Source	Site	Sample	(approximate) Age or residence time a	Specifications			Soil formation (production) rate t/km²/a
A) Alpine climate							
Anderson et al., 2000				Chemical weathering (t/km²/a) [1)]	Erosion (t/km²/a) [2)]		
	seep 13		50	118.0	118.0		235.9
	seep 14		50	124.8	124.8		249.5
	pond		50	159.7	159.7		319.5
	stream 5		50	90.1	90.1		180.1
	stream 4		50	97.0	97.0		194.0
	stream 12		50	90.1	90.1		180.2
	stream 3		200	76.0	76.0		152.1
	stream 2		200	69.3	69.3		138.6
	stream 1		400	62.3	62.3		124.6
	stream 10		400	41.5	41.5		82.9
	stream 9		400	48.4	48.4		96.8
	stream 8		400	34.6	34.6		69.1
	stream 7		400	20.7	20.7		41.4
	stream 11		9000	13.8	13.8		27.6
	stream 6		18000	6.8	6.8		13.7
He and Tang, 2008				Soil thickness (cm)	Density (kg/dm³)	Soil skeleton (%)[3)]	
	Profile 2		39	8	1.42	20	2330
	Profile 3		70	25	1.29	20	3697
	Profile 4		98	20	1.18	20	1923
	Profile 5		130	19	1.17	24	1313
	Profile 6		159	18	1.34	38	887
	Profile 7		183	32	1.13	20	1575
Norton et al., 2010							
	Site						
	Ober-R		7900[4)]				115.4
	Ober-R(2)b		8700				97.0
	Ober-Rg		12000				39.2
	Ober-Vg		6400				157.0
	Ober-I		8100				111.6
	Nider-V		5900				178.2
	Nider-Vg		10000				72.2
	Hil-R		11000				53.5
	Hil-I		7800				119.3
	Hil-(2)b		7100				138.4
	Hil-(3)c		9000				91.6
	Wil-R		8600				98.5
	Wil-V		7400				127.6
	Mil-V		8100				111.6

	Mil-Rg		11000				56.0
	Mil-R		10000				67.7
	Bet-V		7200				135.0
	Bet-R		10000				65.5
Goodman et al., 2001				Soil thickness (cm)	Density (kg/dm^3)	Soil skeleton (%)[3]	
	J1		18919[5]	65	1.50	44	29.1
	J2		18919	130	1.50	50	51.0
	J3		17185	80	1.78	57	35.8
	J4		12250	93	1.62	35	77.9
	U1		45890	103	1.73	52	18.5
	U2		17073	84	1.68	41	47.0
	U3		17073	102	1.77	54	47.4
	U4		17073	100	1.61	41	55.3
	U5		2970	97	1.34	24	332.3
	U6		2970	44	1.29	52	91.7
	U7		2970	23	0.85	51	32.2
	U8		398	17	1.40	58	253.9
	M1		18919	82	1.70	52	35.9
	Q1		25460	95	1.56	35	37.1
	Q2		17554	80	1.76	39	48.9
	Q3		14381	34	1.61	40	22.8
	Q4		12764	70	1.67	58	38.6

B) Temperate climate

Heimsath, 2001a				Denudation (m Ma^{-1})			
	Soils	FH-3	34600	18.69			22.4
		FH-10	24600	26.42			31.7
		FH-5	16600	49.08			58.9
		FH-6	16500	49.42			59.3
		FH-9	31200	25.99			31.2
		FH-11	66600	11.79			14.1
		FH-12	70900	11.05			13.3
	Tors	FH-1	115300	5.26			13.9
		FH-2	22800	28.42			75.3
		FH-4	23800	27.31			72.4
		FH-7	40600	15.81			41.9
		FH-8	129900	4.62			12.2
		FH-13	160100	3.65			9.7
		FH-15	162100	3.6			9.5
		FH-16	137400	4.33			11.5
		FH-17	158000	3.71			9.8
		FH-18	160000	3.57			9.5
	Sediments	FH-14	71200	8.8			23.3
		FH-19	41400	15.47			41.0
		FH-20	39200	16.38			43.4
		FH-21	51100	12.45			33.0
		FH-22	71800	8.72			23.1
		FH-25	66400	9.46			25.1

Ma et al., 2010				
	Site		mm/ka	
	SPRT	6700	44.7	67.1
	SPMS	33500	17.6	26.4
	SPVF	39500	17	25.5

[1] Chemical weathering data were transformed into oxide-forms based on the solute concentrations

[2] Potential erosion rates assuming that chemical weathering is approx. ½ total denudation D (mostly in the range of 0.1 – 0.75D; see Dixon and von Blanckenburg, 2012). The potential erosion rates are probably underestimated. Using the approach D = E + W, soil formation could be calculated by $D = D_{soil}$

[3] Soil skeleton content had to be estimated based on the published soil descriptions

[4] Apparent ages

[5] Where possible, radiocarbon ages were recalibrated using the latest version of OxCal (OxCal 4.1calibration program (Bronk Ramsey, 2001; 2009) based on the IntCal 09 calibration curve (Reimer et al., 2009)). The ages are given as average (calculated as the 'average' of the 2σ end-values) that were used for drawing the figure.

Table 4
Click here to download Table: Table4.doc

Table 4. Compiled datasets of soil formation rates in Mediterranean climate zones as a function of time (basic data compilation is given in Sauer, 2010).

Age a	Soil thickness cm	Density kg/dm^3	Soil skeleton (%) %	Mass kg/m^2	Formation rate $t/km^2/yr$	Source	Remarks: density, soil skeleton
500	38	1.40	51	261	521	Alonso et al., 1994; Dorronsoro and Alonso, 1994	no indications about soil density
10000	153	1.40	48	1114	111		
50000	174	1.40	50	1218	24		
100000	103	1.40	30	1009	10		
100000	167	1.40	39	1426	14		
300000	175	1.40	44	1372	5		
500000	193	1.40	44	1513	3		
600000	200	1.40	16	2352	4		
50000	95	1.70	22	1260	25	Alonso et al., 2004	no indications about soil density
400000	150	1.70	22	1989	5		
600000	393	1.70	12	5879	10		
105000	170	1.70	20	2312	22	Aniku and Singer, 1990	no precise information about soil skeleton: marine beach deposits - c. 20%
370000	287	1.65	20	3788	10		
490000	293	1.67	20	3914	8		
600000	205	1.61	20	2640	4		
25	10	1.70	78	37	1496	Badía et al., 2009	no indication about density
1000	30	1.70	0	510	510		
11000	180	1.70	41	1805	164		
49000	50	1.70	45	468	10		
64000	50	1.70	70	255	4		
176000	75	1.70	61	497	3		
780000	165	1.70	75	701	1		
600	41	1.70	0	697	1162	Busacca, 1987	soil skeleton roughly estimated from soil description; no indication about soil density
10000	183	1.70	0	3111	311		
40000	141	1.70	15	2037	51		
130000	223	1.70	0	3791	29		
250000	238	1.70	10	3641	15		
1600000	388	1.70	35	4287	3		
300	32	1.55	3	481	1604	Calero et al., 2008; Calero, 2005	
7000	75	1.53	29	816	117		
70000	183	1.55	9	2587	37		
300000	89	1.51	15	1142	4		
600000	175	1.55	26	2007	3		
1500	130	1.88	0	2444	1629	Eppes et al., 2008	density given by transfer function
5457	168	1.82	0	3049	559		
12525	230	1.78	35	2654	212		
22950	600	1.78	32	7244	316		

120000	144	1.89	0	2727	23		
200000	185	1.88	0	3478	17		
200	12	1.70	50	102	510	Harden, 1982	no further specific data given
3000	35	1.70	40	357	119		
10000	107	1.70	40	1091	109		
40000	201	1.70	30	2392	60		
130000	350	1.70	20	4760	37		
250000	386	1.70	10	5906	24		
330000	197	1.70	10	3014	9		
600000	230	1.70	10	3519	6		
3000000	274	1.70	10	4192	1		
700	60	1.50	0	900	1286	Harden et al., 1986	
2000	101	1.40	0	1414	707		
40000	158	1.70	2	2632	66		
80000	266	1.65	0	4389	55		
275	24	1.70	50	204	742	Harrison et al., 1990	no indication given
7150	33	1.70	40	337	47		
8350	43	1.70	40	439	53		
12400	85	1.70	40	867	70		
7800	46	1.70	40	469	60	Harrison et al., 1990	no indication given
12400	96	1.70	40	979	79		
47	27	1.40	50	189	4021	McFadden and Weldon, 1987	no indication given; estimated also in comparison to Harden et al., 1986
275	26	1.40	50	182	662		
5900	63	1.50	40	567	96		
7800	45	1.50	40	405	52		
11500	59	1.50	30	620	54		
12400	79	1.50	30	830	67		
55000	120	1.70	20	1632	30		
500000	1460	1.70	10	22338	45		
400	17	1.70	5	275	686	Meixner and Singer, 1981	gravel: roughly estimated from soil description; no indication about soil density
3000	25	1.70	5	404	135		
14000	109	1.70	15	1575	113		
70000	96	1.70	5	1550	22		
140000	122	1.70	5	1970	14		
250000	180	1.70	20	2448	10		
3900	115	1.45	0	1668	428	Merrits et al., 1991	no indication about soil density
29000	135	1.50	3	1964	68		
40000	139	1.50	24	1585	40		
124000	251	1.70	4	4096	33		
240000	264	1.80	5	4514	19		
190	44	1.52	0	669	3520	Sauer et al., 2010	
7000	85	1.96	0	1666	238		
80000	240	1.80	18	3542	44		
100000	350	1.90	8	6118	61		
120000	112	1.93	1	2140	18		
195000	223	2.00	3	4326	22		

310000	206	2.20	36	2900	9
405000	182	1.95	50	1775	4
500000	338	1.90	50	3211	6
575000	319	1.90	6	5697	10
670000	230	1.90	2	4283	6

Figure 1
Click here to download high resolution image

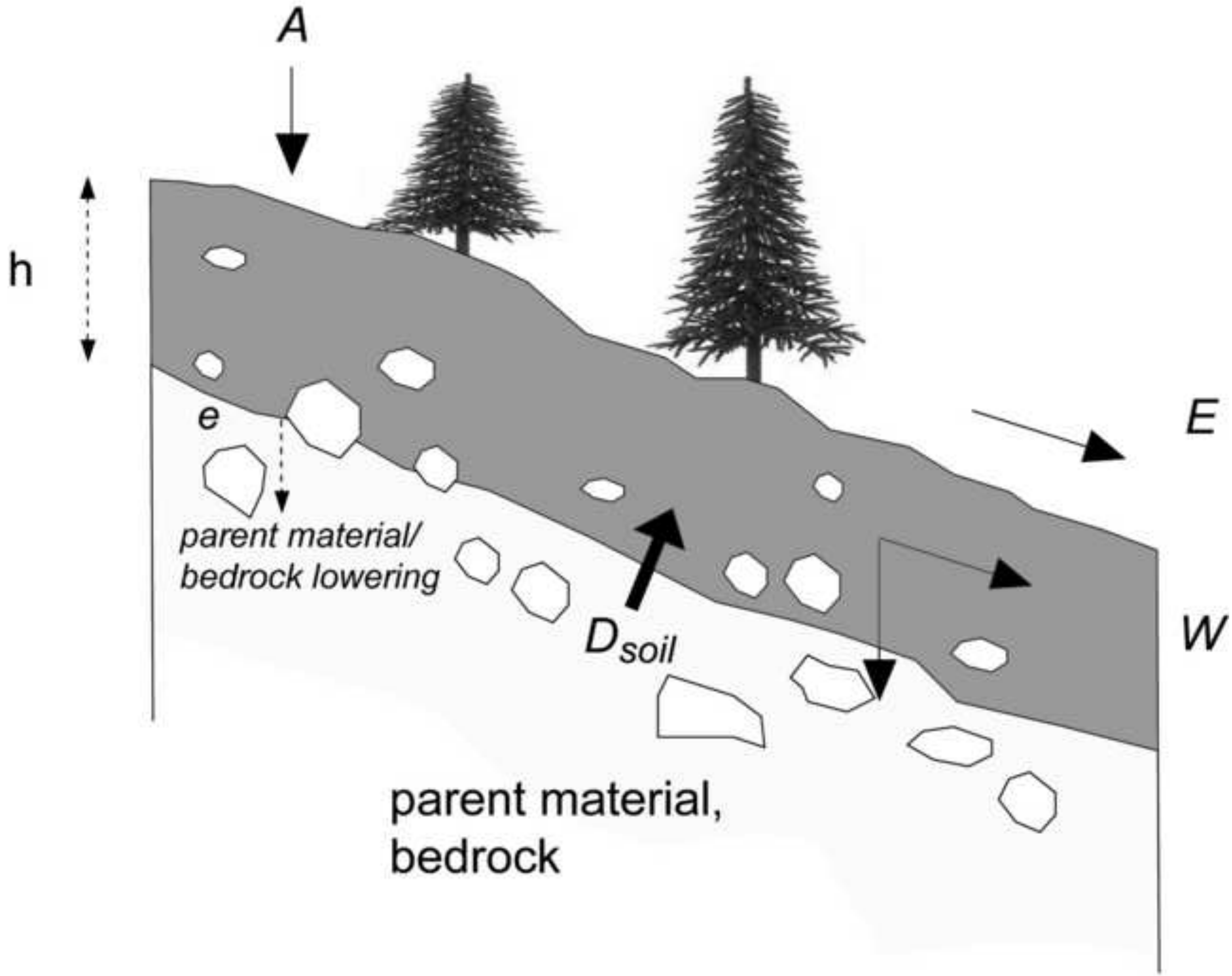

Figure 2
Click here to download high resolution image

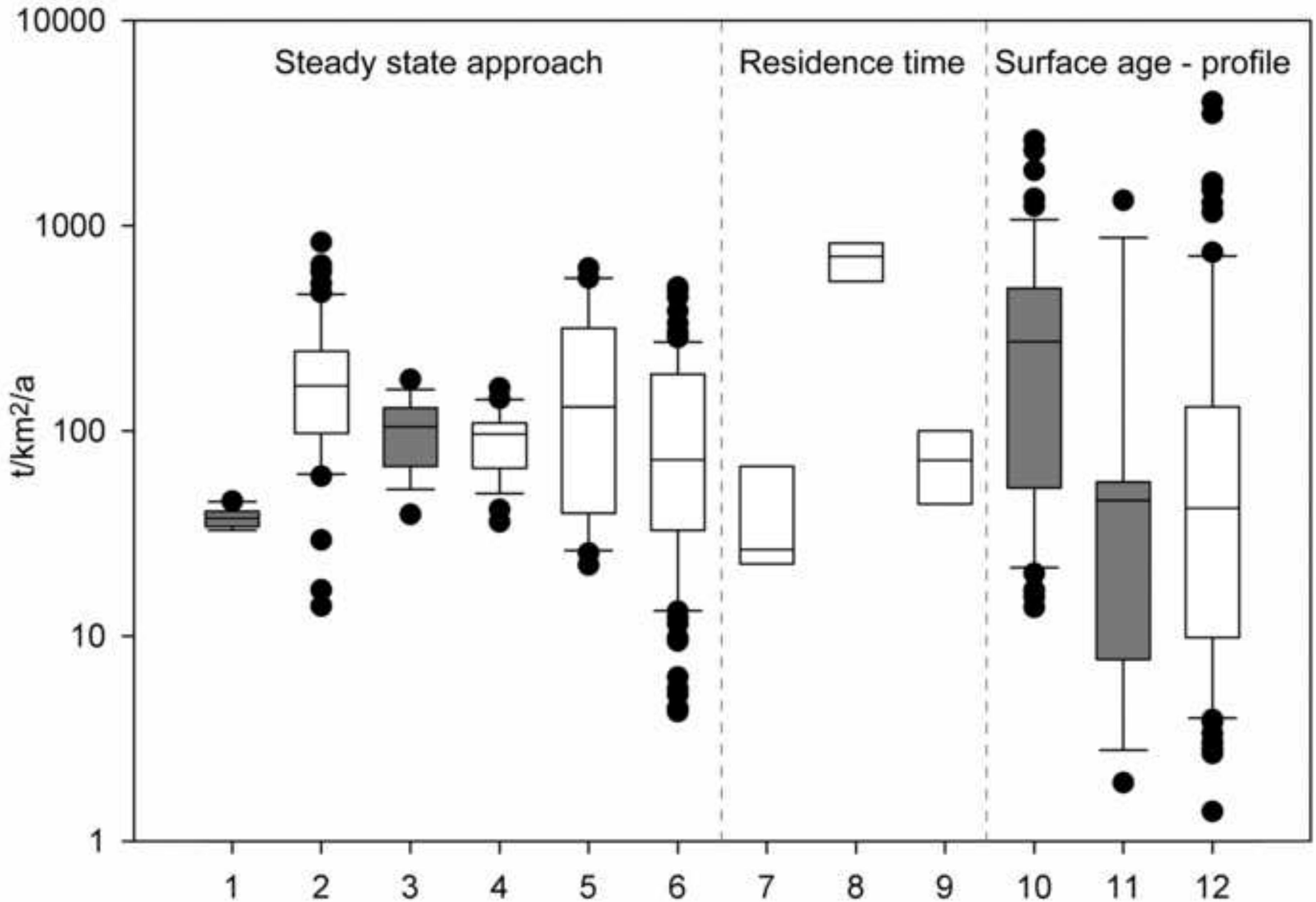

Figure 3
Click here to download high resolution image

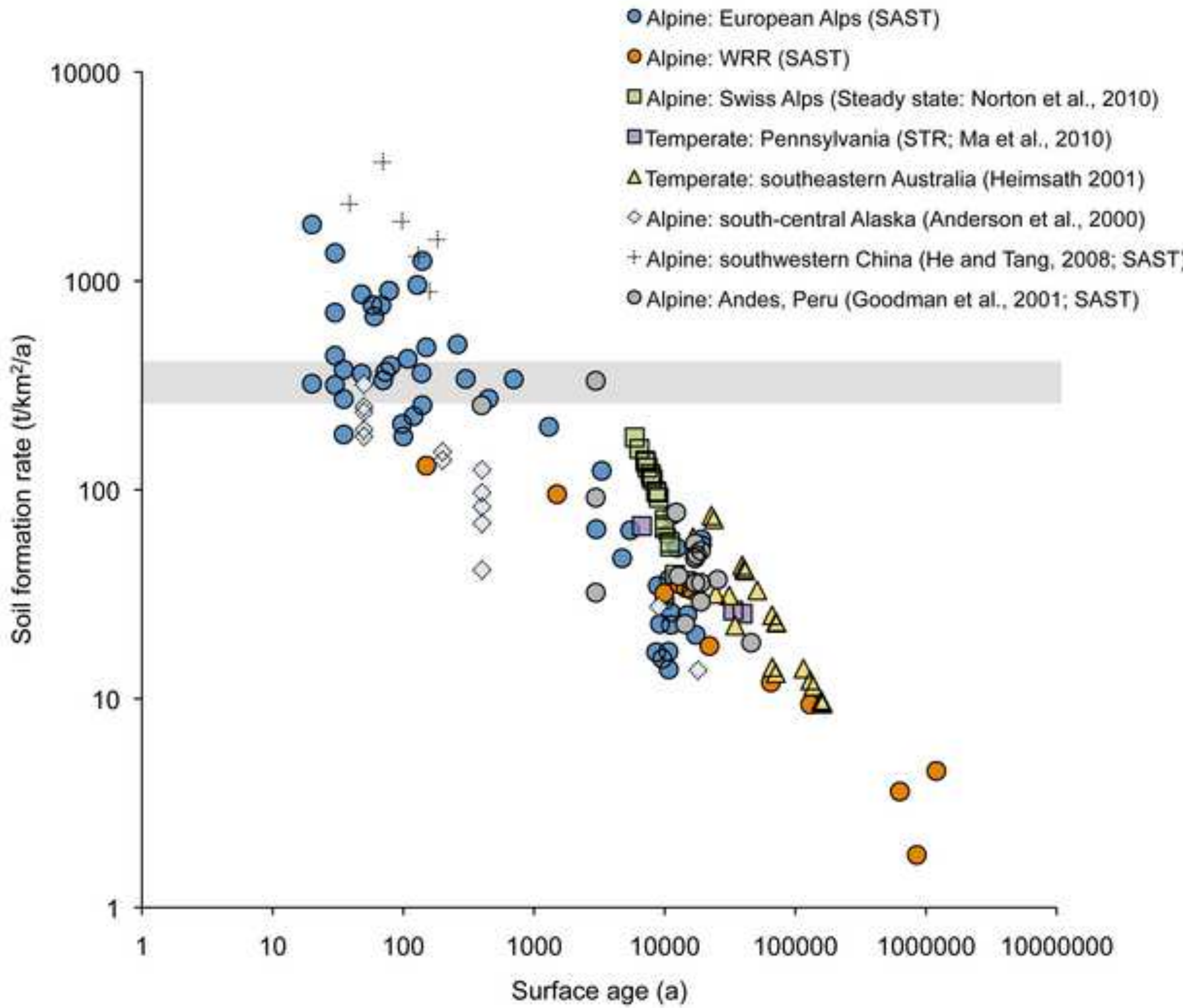

Figure 4
Click here to download high resolution image

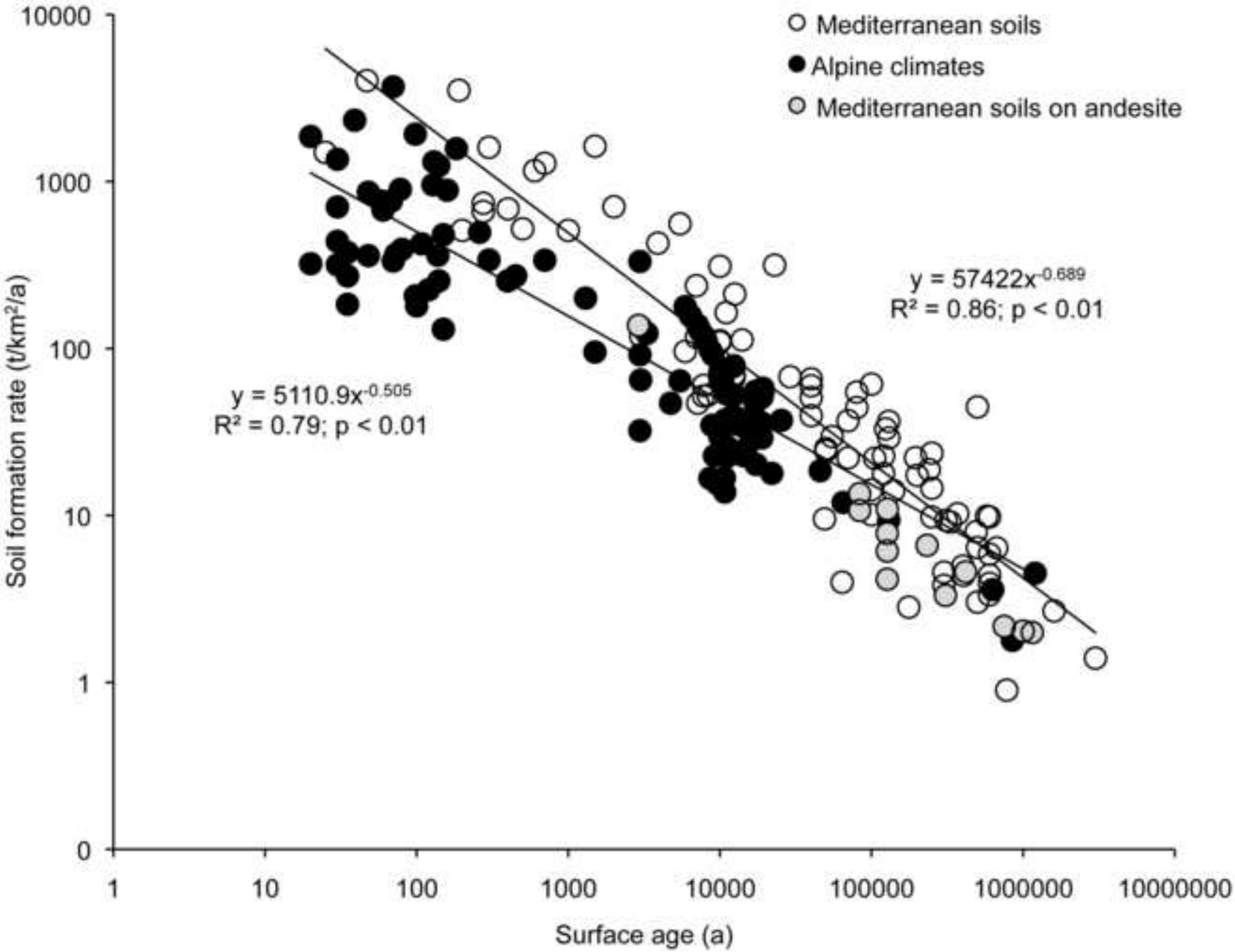

Figure captions

Fig. 1. Schematic overview for the evolution of a soil profile. Symbol e refers to the interface between bedrock (or parent material) and soil; h is the soil thickness. The formation rate is given by D_{soil}. *A*, *E* and *W* correspond to atmospheric input, erosion and chemical weathering (solute output), respectively.

Fig. 2. Comparison of soil formation/production rates based on different approaches (steady state approach using cosmogenic nuclides, residence time using U and Th isotope distribution, surface age and soil profile thickness) and from different climatic regions. Alpine sites (European Alps and Wind River Range) are highlighted in gray.

• 1: Alpine sites of the Wind River Range (Rocky Mountains; Small et al., 1999); n = 10; • 2: San Gabriel Mountains (subtropical to temperate climate zone; Heimsath et al., 2012); n = 54; • 3: Swiss Alps (Norton et al., 2010); n = 18; • 4: Alpine areas (Dixon et al., 2009: Sierra Nevada Mountains (California); Riebe et al., 2004a,b: Santa Rosa Mountains (Nevada), Adams Peak (Sierra Nevada)); n = 25; • 5: Tropical regions (Riebe et al., 2004b: Rio Icacos (Puerto Rico), Chiapas Highlands (Mexico), Jalisco Highlands (Mexico), Jalisco Lowlands (Mexico); Heimsath et al., 2009: Tin Tam Creek (Australia)); n = 21; • 6: Temperate mountain regions (Riebe et al., 2001: Sierra Nevada; Heimsath et al., 2001a,b: Oregon coast region, south-eastern highlands of Australia; Heimsath et al., 2005, 1997: Nunnock River (south-eastern Australia), Tennessee Valley and Mount vision (California); Dixon et al., 2009: Sierra Nevada Mountains (California)), n = 155; • 7: Temperate mountain regions (Dosseto et al., 2008: Nunnock River catchment, Great Diving Range (south-eastern Australia); Dosseto et al., 2011: south-eastern highlands of Australia; Ma et al., 2010: Susquehanna/Shale Hills Observatory (Pennsylvania, USA)); n = 7; • 8: Humid-(sub)tropical mountains (Dosseto et al., 2012: Bisley (Puerto Rico)); n = 3; • 9: Tropical regions (data given in Dosseto et al., 2011, 2012: Mathieu et al., 1995; Dequincey et al., 2002; Dosseto et al., 2007, regions: Brazil, Burkina-Faso, Puerto Rico, Australia, Shale (Pennsylvania, USA)); n = 6; • 10: Italian and Swiss Alps (see Dahms et al., 2012); n = 55; • 11: Wind River Range (WRR) (see Dahms et al., 2012); n = 13; • 12: Mediterranean areas (data compilation according to Sauer, 2010); n = 88.

All data are presented in t/km^2/yr. We converted rates there where presented in length per time units to t/km^2/yr by using the a) the density to calculate the cosmogenic nuclide attenuation depth (when authors did not report this density, we use a value of 2.6 g/cm^3 – Small et al., 1999), b) the given soil densities that were reported by the authors, c) estimated soil densities when no values were given (e.g. 1.6 g/cm^3 for the values reported in Dosseto et al., 2011, 2012 for the (sub)tropical and tropical sites and 1.5g/cm^3 for the sites in a temperate climate).

Fig. 3. Time trends of soil formation in the Wind River Range (WRR) and the Alps (Italian and Swiss Alps) based on the surface age – profile thickness approach. In addition, data from Norton et al. (2010; where 'apparent ages' are presented; alpine climate), Ma et al. (2010; where 'residence times' where given; temperate climate), Heimsath et al. (2001a; temperate climate), He and Tang (2008; alpine climate), Anderson et al. (2000; alpine climate) and Goodman et al. (2001; alpine climate, chronosequence in Peru) are also included. For further explanations, see also Table 2. Gray range: soil production speed limit (according to Dixon and von Blanckenburg, 2012).

Fig. 4. Comparison of soil formation rates using the SAST approach between alpine (and temperate) climates and Mediterranean areas. The regression curve was calculated for the alpine sites without using the sites of Anderson et al. (2000) because soil formation rates are probably underestimated (cf. Table 3). In addition to the site and data compilation of Sauer et al. (2010), soil formation rates at Mediterranean sites having andesite (Muhs, 1982) are plotted. Where possible, the C-14 ages given by Muhs (1982) were recalibrated.